Bull. Mater. Sci., Vol. 31, No. 4, August 2008, pp. 699–711. © Indian Academy of Sciences.

Inhibition of corrosion of mild steel in acid media by N′-benzylidene-3-(quinolin-4-ylthio)propanohydrazide

V RAMESH SALIYAN and AIRODY VASUDEVA ADHIKARI*
Department of Chemistry, National Institute of Technology, Surathkal 575 025, India

MS received 26 November 2007; revised 15 January 2008

Abstract. **In the present investigation a new corrosion inhibitor, N′-(3,4-dihydroxybenzylidene)-3-{[8-(trifluoromethyl)quinolin-4-yl]thio}propanohydrazide(DHBTPH) was synthesized, characterized and tested as a corrosion inhibitor for mild steel in HCl (1 M, 2 M) and H_2SO_4 (0·5 M, 1 M) solutions using weight-loss method, electrochemical impedance spectroscopy (EIS) and potentiodynamic polarization methods. The corrosion inhibition efficiency measured by all the above three techniques were in good agreement with each other. The results showed that DHBTPH is a very good inhibitor for mild steel in acidic media. The inhibition efficiency in different acid media was found to be in the decreasing order 0·5 M H_2SO_4 > 1 M HCl > 1 M H_2SO_4 > 2 M HCl. The inhibition efficiency increases with increasing inhibitor concentration and with increasing temperature. It acts as an anodic inhibitor. Thermodynamic and activation parameters are discussed. Adsorption of DHBTPH was found to follow the Langmuir's adsorption isotherm. Chemisorption mechanism is proposed. The mild steel samples were also analysed by scanning electron microscopy (SEM).**

Keywords. **Activation energy; adsorption isotherms; corrosion inhibitors; mild steel; scanning electron microscopy; thermodynamic parameters.**

1. Introduction

Acid corrosion inhibitors find vast application in the industrial field as components in acid descaling, oil well acidizing, acid pickling, acid cleaning, etc. Most of the efficient corrosion inhibitors used in industry are organic compounds having multiple bonds and hetero atoms like N, O, S through which they are adsorbed on the metal surface (Rengamani *et al* 1994; Abd El-Rehim *et al* 1999; Quraishi and Jamal 2002; Emregul *et al* 2003; Khaled *et al* 2004; Wang *et al* 2004; Bentiss *et al* 2005; Zor *et al* 2005). The influence of such organic compounds on the corrosion of mild steel in acidic solution has been investigated by several researchers (Quraishi *et al* 2002; Popova *et al* 2004; Vishwanatham and Anil Kumar 2005). The inhibition property of these compounds is attributed to their molecular structure (Mora-Mendoza *et al* 2002).

The aim of this work was to investigate the role played by newly synthesized N′-(3,4-dihydroxybenzylidene)-3-{[8-(trifluoromethyl)quinolin-4-yl]thio}propanohydrazide (DHBTPH) on the corrosion behaviour of mild steel in HCl (1 M, 2 M) and H_2SO_4 (0·5 M, 1 M) solutions. The molecular design of the new compound was based on the fact that quinoline (a nitrogen heterocycle) containing trifluoromethyl group, thio, hydroxy and hydrazide groups would contribute more effectively towards inhibition of corrosion of mild steel in acidic media.

In view of this, a new inhibitor, DHBTPH (**2**) was synthesized, characterized and the inhibitive action of it on the corrosion behaviour of mild steel in acid media was measured. Corrosion inhibition was investigated using weight-loss, electrochemical impedance spectroscopic (EIS) and potentiodynamic polarization (Tafel) methods and their results were compared.

2. Experimental

2.1 *Inhibitor synthesis and characterization*

A mixture of 3·15 g (0·01 mol) of 3-{[8-(trifluoromethyl) quinolin-4-yl]thio} propane hydrazide (**1**), 1·66 g of 3,4-dihydroxy benzaldehyde (0·012 mol), 0·2 mL of glacial acetic acid and 25 mL of dry methanol was refluxed for 8 h. The crystalline product thus obtained was filtered, washed, dried and re-crystallized in ethanol to afford the crystals of **2**, yield 91% and m.p. 188–190°C. The required intermediates were prepared following reported procedures (Allais *et al* 1969). Their purity was monitored by thin layer chromatography, and its structure was established by spectral and elemental analyses. Scheme 1 shows the synthesis sequence. The IR spectra (in KBr pellets) were recorded on a Thermo-Avatar spectrophotometer. Mass spectra were recorded on a Jeol JMS-D 300 operating at

*Author for correspondence (avchem@nitk.ac.in)

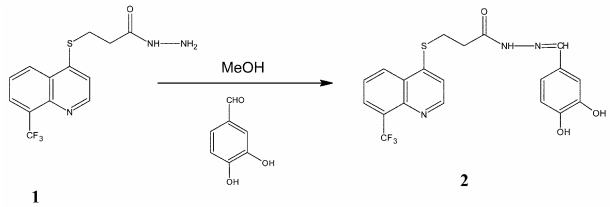

Scheme 1.

70 eV. Thermo Electron Corporation Flash EA 1112 series CHN analyser was used for elemental analysis.

2.2 *Corrosion and its inhibition studies*

Mild steel specimen of chemical composition, C 0·16%, Mn 0·2%, S 0·05%, P 0·07%, Si 0·2% and the remainder iron, in sheet form have been used for weight-loss measurements. The samples were polished with different emery papers of grades 0, 1, 2, 3 and 4, cleaned with acetone, washed with doubly distilled water and finally dried. For the electrochemical measurement the arrangement used was a conventional three-electrode Pyrex glass cell with a platinum counter electrode and a saturated calomel electrode (SCE) as reference. The working steel specimen cut from cylindrical rods of mild steel was covered with epoxy adhesive—Araldite, so that its cross sectional area, 0·785 cm^2, was in contact with the solution. Experiments were carried out at constant temperature of ± 0·5°C using a calibrated thermostat. The solutions for all the experiments were prepared with doubly distilled water, analar grade hydrochloric acid (Merck) and sulphuric acid (Merck).

For weight-loss measurements, a clean weighed mild steel specimen in the sheet form (2 × 5 × 0·05 cm) was completely immersed at inclined position in a beaker. After 24 h of immersion, the electrode was withdrawn, rinsed with doubly distilled water, washed with acetone, dried and weighed. The weight-loss was used to calculate the corrosion rate (CR) in milligrams per square centimetre per hour.

EIS and Tafel polarization studies were carried out by using an electrochemical work station (Auto Lab 30, Metrohm). EIS measurements were carried out in a frequency range of 1,00,000 Hz–0·05 Hz using an amplitude of 10 mV, peak-to-peak using a.c. signal at the open circuit potential. The potentiodynamic current–potential curves were recorded by changing the electrode potential automatically from – 250 mV to + 250 mV vs OCP with a scan rate of 1 mV s^{-1}. Polished mild steel specimen of 0·785 cm^2 surface area was exposed to 100 mL of HCl (1 M, 2 M) and H_2SO_4 (0·5 M, 1 M) solutions at 30°C without and with various concentrations ($0{\cdot}230 \times 10^{-4}$ to $11{\cdot}494 \times 10^{-4}$ M) of inhibitors. Similar experiments were carried out at 40°, 50° and 60°C.

The electrode surface was examined by making photographs of the surface. SEM Jeol JSM-6380 was used for this purpose.

3. Results and discussion

3.1 *Characterization of DHBTPH* **2**

The characterization data of N′-(3,4-dihydroxybenzylidene)-3-{[8-(trifluoromethyl) quinolin-4-yl]thio}propanohydrazide (DHBTPH, **2**) are given below.

IR: (KBr) ν cm^{-1}: 3437·4 (N–H str.), 3274 (O–H), 2961·7 (C–H), 1654·1 (C=O), 1577·7 (C=N), 1518·3 (N–H bending), 1148·6, 1097·8, 1021·8 (C–F), 700·4 (C–S).

MASS (M^+): The molecular ion peak (M^+) appeared at 435, which corresponds to its molecular formula, $C_{20}H_{16}F_3N_3O_3S$, confirming the formation of compound **2**. The base peak appearing at 436 is due to protonated molecular ion peak $(M + H)^+$, the presence of which confirms the structure of **2**.

Elemental analysis: Found (calcd): C, 55·25 (55·22); H, 3·69 (3·71); N, 9·68 (9·66) %; $C_{20}H_{16}F_3N_3O_3S$.

3.2 *Corrosion measurement*

3.2a *Weight-loss method*: The weight-loss of mild steel strips in 100 mL of HCl (1 M, 2 M) and H_2SO_4 (0·5 M, 1 M) solutions at 30°C without and with various concentrations ($0{\cdot}230 \times 10^{-4}$ to $11{\cdot}494 \times 10^{-4}$ M) of inhibitors were determined after 24 h of immersion period. The inhibition efficiency, %*IE*, was determined by using the following equation

$$\%IE = \frac{W_{\text{corr}} - W_{\text{corr(inh)}}}{W_{\text{corr}}} \times 100, \quad (1)$$

where W_{corr} and $W_{\text{corr(inh)}}$ are the corrosion rates of mild steel in the absence and presence of the inhibitor, respectively. The values of *%IE* and corrosion rate (CR) obtained from weight-loss measurements for different acids and different inhibitor concentrations at 30°C are given in table 1.

Corrosion inhibition efficiency increases with increasing concentration of inhibitor in all the four acid media (table 1). The corrosion inhibition efficiency trend in different acid media was in the decreasing order 0·5 M H_2SO_4 > 1 M HCl > 1 M H_2SO_4 > 2 M HCl. The higher %*IE* in H_2SO_4 than HCl may be due to the availability of more sites on the metal surface in H_2SO_4 solution because of the lesser adsorption of the sulphate ion on the steel surface (Bentiss *et al* 2001). In each acid media, maximum *%IE* was achieved at $11{\cdot}494 \times 10^{-4}$ M and a further increase in concentration did not cause any appreciable change in the performance of the inhibitor. The corrosion inhibition can be attributed to the adsorption of the inhibitor at the steel/acid solution interface. The adsorption is mainly attributed to higher electron densities at active functional groups, present in the DHBTPH molecules (Bentiss *et al* 2005).

3.2b *EIS method*: EIS technique was also used to investigate the corrosion behaviour of mild steel in all the

Table 1. Corrosion parameters obtained from weight-loss and electrochemical measurements of mild steel in acid media containing various concentrations of DHBTPH at 30°C.

Acid media	Inhibitor conc. (10^{-4} M)	Weight-loss		EIS			Polarization curves	
		CR (mg cm^{-2} h^{-1})	*IE* (%)	R_t (Ωcm^{-2})	C_{dl} ($\mu F cm^{-2}$)	*IE* (%)	I_{corr} ($\mu A cm^{-2}$)	*IE* (%)
1 M HCl	Blank	2·15	–	24·54	260·2	–	570	–
	0·230	1·32	38·5	37·52	195·2	34·6	360	36·8
	1·149	1·04	51·7	47·10	145·6	47·9	287	49·7
	2·299	0·76	64·5	62·44	130·1	60·7	213	62·6
	5·747	0·48	77·5	92·26	115·7	73·4	140	75·5
	11·494	0·21	90·2	177·83	96·3	86·2	066	88·4
2 M HCl	Blank	3·87	–	14·63	280·9	–	941	–
	0·230	2·30	40·5	23·26	205·6	37·1	575	38·9
	1·149	1·83	52·6	28·46	165·2	48·6	465	50·6
	2·299	1·37	64·6	37·61	142·3	61·1	349	62·9
	5·747	0·92	76·2	53·20	125·1	72·5	240	74·5
	11·494	0·53	86·4	83·13	110·8	82·4	146	84·5
0·5 M H_2SO_4	Blank	4·52	–	12·55	240·5	–	1083	–
	0·230	1·64	63·7	31·38	188·4	60·0	412	62·0
	1·149	1·36	70·0	37·13	146·8	66·2	344	68·2
	2·299	0·97	78·6	50·20	120·3	75·0	249	77·0
	5·747	0·63	86·1	70·90	102·7	82·3	170	84·3
	11·494	0·16	96·4	171·92	85·6	92·7	057	94·7
1 M H_2SO_4	Blank	9·68	–	6·18	290·6	–	2138	–
	0·230	4·00	58·7	13·83	205·3	55·3	915	57·2
	1·149	3·30	65·9	16·44	165·9	62·4	759	64·5
	2·299	2·57	73·5	20·46	140·7	69·8	603	71·8
	5·747	1·83	81·1	27·11	125·6	77·2	447	79·1
	11·494	1·18	87·8	39·87	106·7	84·5	291	86·4

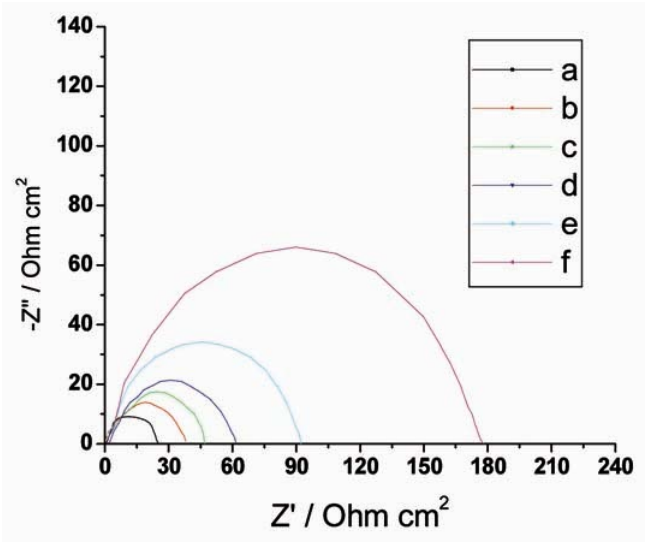

Figure 1. Complex-plane impedance of mild steel in 1 M HCl at 30°C in presence of different concentrations of DHBTPH: (a) 0, (b) $0·230 \times 10^{-4}$, (c) $1·149 \times 10^{-4}$, (d) $2·299 \times 10^{-4}$, (e) $5·747 \times 10^{-4}$ and (f) $11·494 \times 10^{-4}$ M.

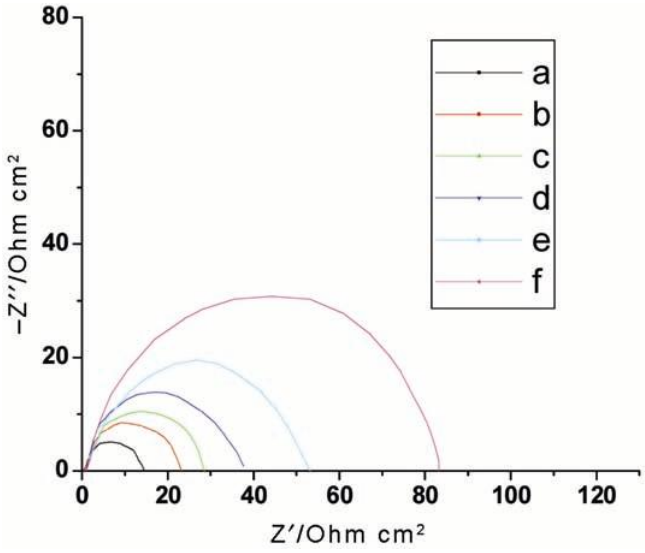

Figure 2. Complex-plane impedance of mild steel in 2 M HCl at 30°C in presence of different concentrations of DHBTPH: (a) 0, (b) $0·230 \times 10^{-4}$, (c) $1·149 \times 10^{-4}$, (d) $2·299 \times 10^{-4}$, (e) $5·747 \times 10^{-4}$ and (f) $11·494 \times 10^{-4}$ M.

above conditions. The equivalent circuit models used to fit the experimental results were as previously reported (Abd El-Rehim *et al* 1999). Figures 1–4 show the complex-plane impedance plots (Nyquist plots) for mild steel in 1 M HCl, 2 M HCl, 0·5 M H_2SO_4 and 1 M H_2SO_4 without and with various concentrations of DHBTPH at 30°C. As it can be seen from the figures, the Nyquist plots contain depressed semi-circle with the centre under the real axis,

whose size increases with the inhibitor concentration, indicating a charge transfer process mainly controlling the corrosion of mild-steel. Such a behaviour, characteristic for solid electrodes and often refer to a frequency dispersion, has been attributed to roughness and other inhomogeneities of the solid surface (Juttner 1990; Stoynov *et al* 1991). It is apparent from these plots that the impedance response of mild steel in uninhibited acid solution has significantly changed after the addition of DHBTPH in the corrosive solutions. This indicated that the impedance of the inhibited substrate has increased with increasing concentration of inhibitor. The characteristic parameters associated to the impedance diagrams (R_t and C_{dl}) and *%IE* are given in table 1. *%IE* was calculated from the following equation

$$\%IE = \frac{\left(\frac{1}{R_t}\right)_0 - \left(\frac{1}{R_t}\right)}{\left(\frac{1}{R_t}\right)_0} \times 100, \quad (2)$$

where $(R_t)_0$ and (R_t) are the uninhibited and inhibited charge transfer resistances, respectively (Abd El-Rehim *et al* 1999). The values of *%IE* obtained from EIS and weight-loss measurements are in sequence.

The R_t values increased with the increasing concentration of the inhibitor (table 1). On the other hand, the value of C_{dl} decreased with an increase in inhibitor concentration. This situation was the result of increase in the surface coverage by the DHBTPH, which led to an increase in the inhibition efficiency (table 1). The thickness of the protective layer, δ_{org}, was related to C_{dl} by the following equation (Bentiss *et al* 2002)

$$\delta_{org} = \frac{\varepsilon_0 \varepsilon_T}{C_{dl}}, \quad (3)$$

where ε_0 is the vacuum dielectric constant and ε_T the relative dielectric constant. This decrease in C_{dl}, which can result from a decrease in local dielectric constant and/or an increase in the thickness of the electrical double layer, suggested that the DHBTPH molecules function by adsorption at the metal/solution interface. Here, the gradual replacement of water molecules by the adsorption of the organic molecules on the metal surface, decreases the extent of metal dissolution and hence it causes the change in C_{dl} values (McCafferty and Hackerman 1972).

Two modes of adsorption can be considered. The process of physical adsorption requires the presence of electrically charged metal surface and the charged species in the bulk of the solution. Chemisorption process involves charge sharing or charge transfer from the inhibitor molecules to the metal surface. This is possible in case of positive as well as negative charges on the surface. The presence of a transition metal, having vacant, low-energy electron orbital, and an inhibitor molecule having relatively loosely bound electrons or hetero atoms with lone-pair electrons facilitates this adsorption (Reinhard and Rammet 1985; Mehaute and Grepy 1989). On the other hand, the DHBTPH, which possesses nitrogen sulphur and oxygen atoms with lone-pair electrons, can accept a proton, leading the cationic forms. These species can adsorb on the metal surface because of attractive forces between the negatively charged metal and the positively charged DHBTPH.

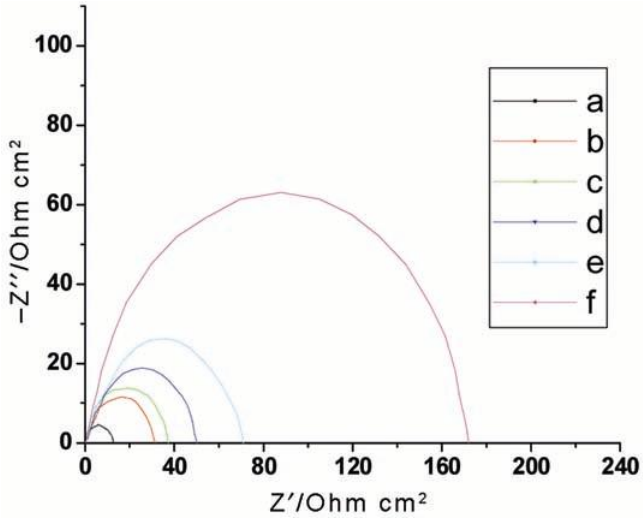

Figure 3. Complex-plane impedance of mild steel in 0·5 M H_2SO_4 at 30°C in presence of different concentrations of DHBTPH: (a) 0, (b) $0{\cdot}230 \times 10^{-4}$, (c) $1{\cdot}149 \times 10^{-4}$, (d) $2{\cdot}299 \times 10^{-4}$, (e) $5{\cdot}747 \times 10^{-4}$ and (f) $11{\cdot}494 \times 10^{-4}$ M.

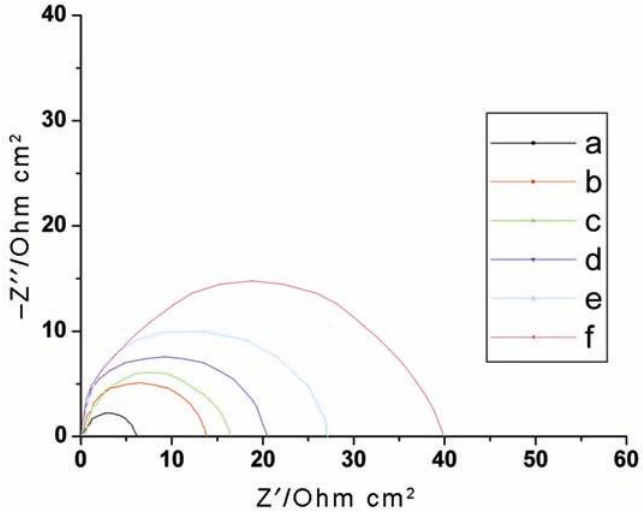

Figure 4. Complex-plane impedance of mild steel in 1 M H_2SO_4 at 30°C in presence of different concentrations of DHBTPH: (a) 0, (b) $0{\cdot}230 \times 10^{-4}$, (c) $1{\cdot}149 \times 10^{-4}$, (d) $2{\cdot}299 \times 10^{-4}$, (e) $5{\cdot}747 \times 10^{-4}$ and (f) $11{\cdot}494 \times 10^{-4}$ M.

3.2c *Tafel polarization method*: As shown in figures 5–8, both cathodic and anodic corrosion reactions of mild

steel were inhibited with the increase of DHBTPH concentration in all corrosive solutions. DHBTPH suppressed the anodic reaction to greater extents than the cathodic one, at all concentrations. This result suggests that the addition of DHBTPH reduces anodic dissolution and also retards the hydrogen evolution reaction. Tafel lines of nearly equal slopes were obtained, indicating that the hydrogen evolution reaction was activation-controlled.

The corrosion current density (I_{corr}) values are presented in table 1. The data show that the I_{corr} values decreased considerably in the presence of DHBTPH and decreased with increasing inhibitor concentration. The decrease in I_{corr} with increasing inhibitor concentration was associated with the shift of corrosion potential, E_{corr}, to a less negative value. This indicates that DHBTPH suppressed anodic reaction. Corrosion inhibition efficiency was calculated using the electrochemical relation

$$\%IE = \frac{[I_{corr} - I_{corr(inh)}]}{I_{corr}} \times 100, \quad (4)$$

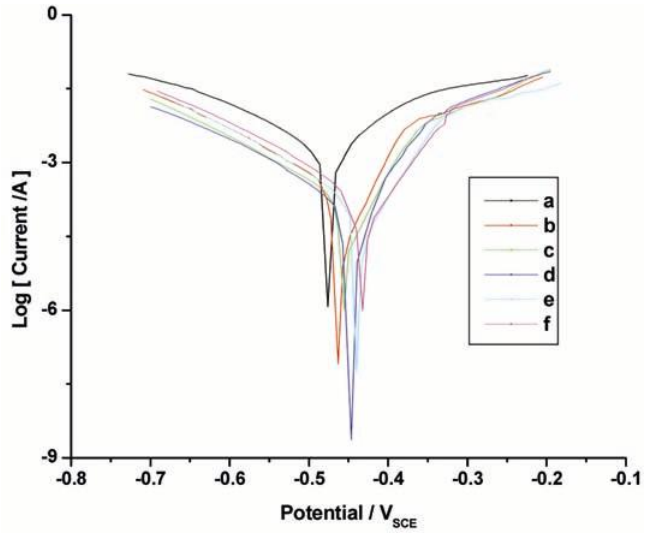

Figure 5. Polarization curves of mild steel in 1 M HCl at 30°C in presence of different concentrations of DHBTPH: (a) 0, (b) $0{\cdot}230 \times 10^{-4}$, (c) $1{\cdot}149 \times 10^{-4}$, (d) $2{\cdot}299 \times 10^{-4}$, (e) $5{\cdot}747 \times 10^{-4}$ and (f) $11{\cdot}494 \times 10^{-4}$ M.

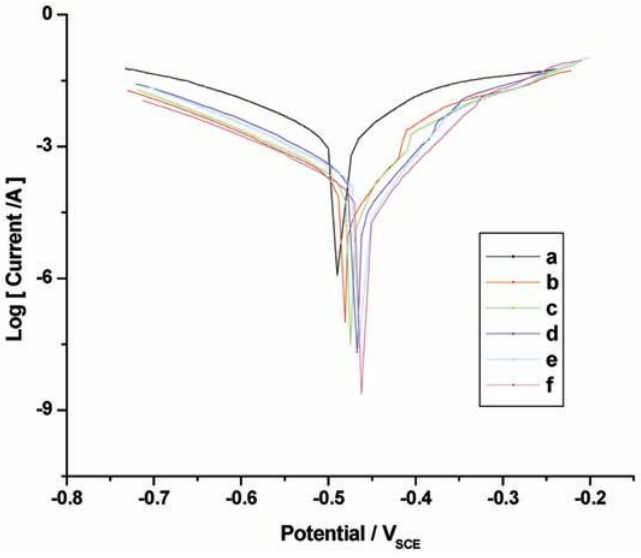

Figure 7. Polarization curves of mild steel in 0·5 M H_2SO_4 at 30°C in presence of different concentrations of DHBTPH: (a) 0, (b) $0{\cdot}230 \times 10^{-4}$, (c) $1{\cdot}149 \times 10^{-4}$, (d) $2{\cdot}299 \times 10^{-4}$, (e) $5{\cdot}747 \times 10^{-4}$ and (f) $11{\cdot}494 \times 10^{-4}$ M.

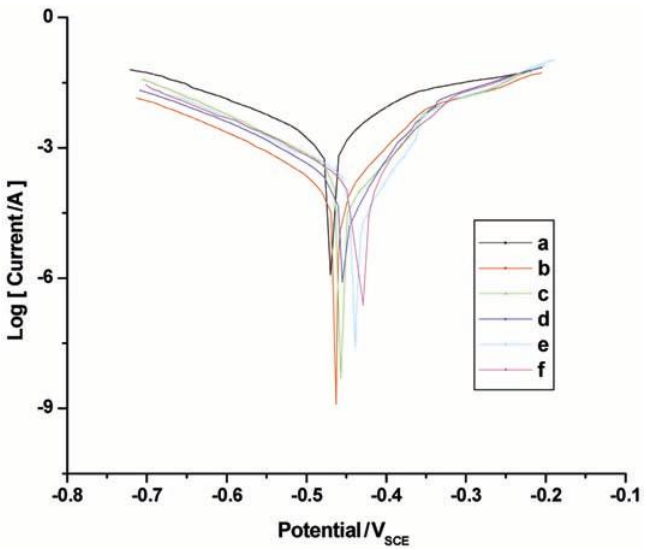

Figure 6. Polarization curves of mild steel in 2 M HCl at 30°C in presence of different concentrations of DHBTPH: (a) 0, (b) $0{\cdot}230 \times 10^{-4}$, (c) $1{\cdot}149 \times 10^{-4}$, (d) $2{\cdot}299 \times 10^{-4}$, (e) $5{\cdot}747 \times 10^{-4}$ and (f) $11{\cdot}494 \times 10^{-4}$ M.

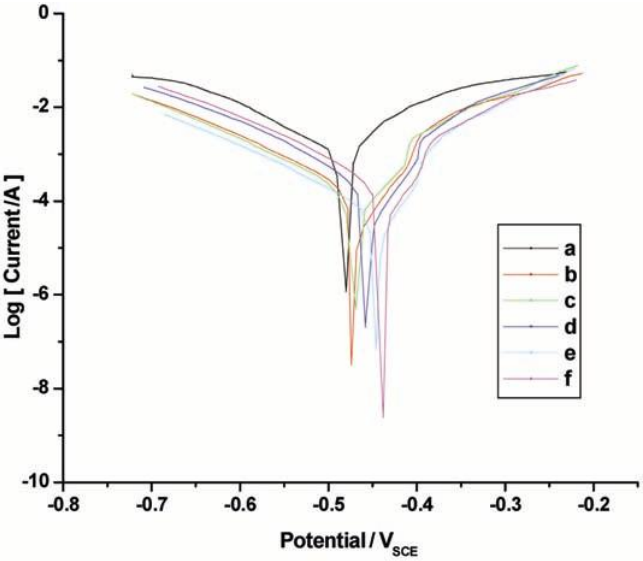

Figure 8. Polarization curves of mild steel in 1 M H_2SO_4 at 30°C in presence of different concentrations of DHBTPH: (a) 0, (b) $0{\cdot}230 \times 10^{-4}$, (c) $1{\cdot}149 \times 10^{-4}$, (d) $2{\cdot}299 \times 10^{-4}$, (e) $5{\cdot}747 \times 10^{-4}$ and (f) $11{\cdot}494 \times 10^{-4}$ M.

Table 2. Electrochemical parameters and the corresponding inhibition efficiencies at various temperatures studied for mild steel in 1 M HCl containing different concentrations of DHBTPH.

Temp. (°C)	Inhibitor conc. (10^{-4} M)	E_{corr} vs SCE (mV)	I_{corr} (μAcm^{-2})	*IE* (%)	θ
30	1 M HCl	–476	570	–	–
	0·230	–463	360	36·8	0·368
	1·149	–455	287	49·7	0·497
	2·299	–446	213	62·6	0·626
	5·747	–440	140	75·5	0·755
	11·494	–432	066	88·4	0·884
40	1 M HCl	–464	912	–	–
	0·230	–455	555	39·1	0·391
	1·149	–442	440	51·8	0·518
	2·299	–439	324	64·5	0·645
	5·747	–425	208	77·2	0·772
	11·494	–423	092	89·9	0·899
50	1 M HCl	–456	1767	–	–
	0·230	–447	995	43·7	0·437
	1·149	–441	779	55·9	0·559
	2·299	–434	564	68·1	0·681
	5·747	–425	348	80·3	0·803
	11·494	–412	133	92·5	0·925
60	1 M HCl	–439	2964	–	–
	0·230	–432	1458	50·8	0·508
	1·149	–426	1132	61·6	0·616
	2·299	–421	806	72·2	0·722
	5·747	–417	480	83·5	0·835
	11·494	–407	169	94·3	0·943

where I_{corr} and $I_{corr(inh)}$ are the corrosion current density values without and with inhibitor, respectively obtained by extrapolation of cathodic and anodic lines to the corrosion potentials.

The %*IE* values obtained from Tafel polarization measurements are tabulated in table 1. These results are comparable with those calculated from weight-loss measurement and EIS measurements. But a little difference was observed. This difference can be attributed to the fact that the gravimetric method gives average corrosion rates, whereas the polarization method gives instantaneous corrosion rates (Muralidharan *et al* 1995; Foad and Sherbini 1999).

3.3 *Effect of temperature*

The effect of temperature on inhibition reaction is highly complex, because many changes may occur on the metal surface such as rapid etching, rupture, desorption of inhibitor and the decomposition and/or rearrangement of inhibitor. The effect of temperature on the rate of corrosion process was studied in different acid media without and with various concentrations of DHBTPH. The present study was aimed at exploring the activation energy of the corrosion process and thermodynamic functions of adsorption of DHBTPH. This was accomplished by investigating the temperature dependence of the corrosion current that was obtained using Tafel extrapolation method. The various electrochemical parameters were calculated from Tafel plots and summarized in tables 2–5. The %*IE* and the degree of surface coverage (θ) for steel are also given in these tables. The degree of surface coverage (θ) was calculated from the following equation (Khamis 1990)

$$\theta = \frac{I_{corr} - I_{corr(inh)}}{I_{corr}}, \tag{5}$$

where I_{corr} and $I_{corr(inh)}$ are the corrosion current density values in the absence and presence of DHBTPH.

The investigated DHBTPH showed inhibiting properties at all the studied temperatures (30–60°C). The values of %*IE* for DHBTPH increased with increase in temperature (tables 2–5). Thus, DHBTPH efficiencies were temperature dependent. Similar observations were discussed by several researchers (Ammar and Khorafi 1973; Ivanov 1986).

The activation parameters for the corrosion process were calculated from Arrhenius-type plot according to the following equation

$$I_{corr} = k \exp\left(-\frac{E_a}{RT}\right), \tag{6}$$

where E_a is the apparent activation corrosion energy, R the universal gas constant and k the Arrhenius pre-exponential constant. Arrhenius plots for the corrosion density of mild steel in the case of DHBTPH in 1 M HCl media are given in figure 9. Values of apparent activation energy of corrosion (E_a) for mild steel in 1 M HCl with the absence

Table 3. Electrochemical parameters and the corresponding inhibition efficiencies at various temperatures studied for mild steel in 2 M HCl containing different concentrations of DHBTPH.

Temp. (°C)	Inhibitor conc. (10^{-4} M)	E_{corr} vs SCE (mV)	I_{corr} (μAcm^{-2})	*IE* (%)	θ
30	2 M HCl	–470	941	–	–
	0·230	–463	575	38·9	0·389
	1·149	–457	465	50·6	0·506
	2·299	–455	349	62·9	0·629
	5·747	–439	240	74·5	0·745
	11·494	–429	146	84·5	0·845
40	2 M HCl	–442	1787	–	–
	0·230	–434	1074	39·9	0·399
	1·149	–430	861	51·8	0·518
	2·299	–426	654	63·4	0·634
	5·747	–421	443	75·2	0·752
	11·494	–418	264	85·2	0·852
50	2 M HCl	–433	3856	–	–
	0·230	–427	2244	41·8	0·418
	1·149	–423	1828	52·6	0·526
	2·299	–418	1361	64·7	0·647
	5·747	–415	910	76·4	0·764
	11·494	–409	536	86·1	0·861
60	2 M HCl	–426	5925	–	–
	0·230	–423	3306	44·2	0·442
	1·149	–419	2625	55·7	0·557
	2·299	–416	1943	67·2	0·672
	5·747	–412	1250	78·9	0·789
	11·494	–400	693	88·3	0·883

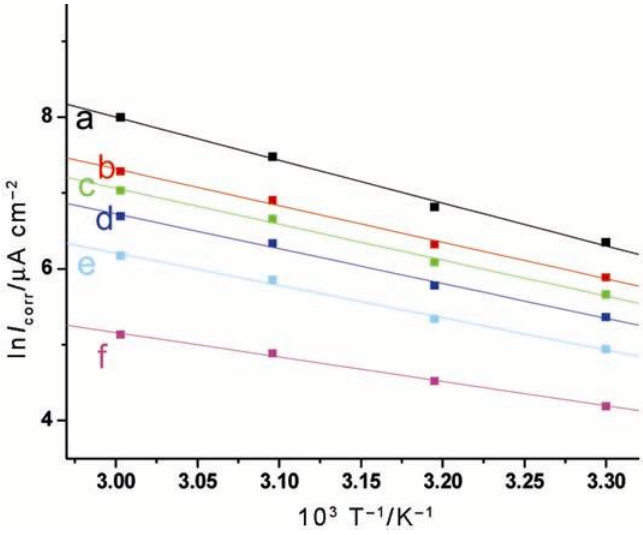

Figure 9. Arrhenius plots of corrosion lnI_{corr} vs 1/T at different concentrations of DHBTPH: (a) 1 M HCl, (b) 1 M HCl + 0·230 × 10^{-4}, (c) 1 M HCl + 1·149 × 10^{-4}, (d) 1 M HCl + 2·299 × 10^{-4}, (e) 1 M HCl + 5·747 × 10^{-4} and (f) 1 M HCl + 11·494 × 10^{-4} M.

and presence of various concentrations of DHBTPH were determined from the slope of ln(I_{corr}) vs 1/T plots and tabulated in table 6. Similarly, E_a values for mild steel in different acid media with the absence and presence of various concentrations of DHBTPH were determined and tabulated in table 6. Inspection of the data shows that the activation energy is lower in the presence of inhibitors than in its absence. Moreover, the values obtained for DHBTPH in 2 M HCl are somewhat higher than those obtained for DHBTPH in 1 M HCl and confirm the fact that the inhibitor efficiency of DHBTPH in 2 M HCl is slightly lower than that in 1 M HCl. Similar trend is observed between 0·5 M H_2SO_4 and 1 M H_2SO_4. The decrease in E_a with DHBTPH concentration (table 6) is typical of chemisorption.

An alternative formulation of Arrhenius equation is (Bentiss *et al* 2005)

$$I_{corr} = \frac{RT}{Nh}\exp\left(\frac{\Delta S_a^0}{R}\right)\exp\left(-\frac{\Delta H_a^0}{RT}\right), \quad (7)$$

where h is Planck's constant, N the Avogadro's number, ΔS_a^0 the entropy of activation and ΔH_a^0 the enthalpy of activation. Figure 10 shows a plot of ln(I_{corr}/T) against 1/T in the case of DHBTPH in 1 M HCl. Similar behaviour is observed in the case of DHBTPH in 2 M HCl, 0·5 M H_2SO_4 and 1 M H_2SO_4. Straight lines are obtained with a slope ($-\Delta H_a^0/R$) and an intercept ($\ln(R/Nh) + \Delta S_a^0/R$) from which the values of ΔH_a^0 and ΔS_a^0 can be calculated (table 6). The positive signs of the enthalpies (ΔH_a^0) reflect the endothermic nature of dissolution process of steel. Large and negative value of entropies (ΔS_a^0) imply that the activated complex in the rate determining step represents an association rather than a dissociation step, meaning that a

Table 4. Electrochemical parameters and the corresponding inhibition efficiencies at various temperatures studied for mild steel in 0·5 M H_2SO_4 containing different concentrations of DHBTPH.

Temp. (°C)	Inhibitor conc. (10^{-4} M)	E_{corr} vs SCE (mV)	I_{corr} (μAcm^{-2})	*IE* (%)	θ
30	0·5 M H_2SO_4	–490	1083	–	–
	0·230	–481	412	62·0	0·620
	1·149	–475	344	68·2	0·682
	2·299	–467	249	77·0	0·770
	5·747	–465	170	84·3	0·843
	11·494	–462	057	94·7	0·947
40	0·5 M H_2SO_4	–469	1949	–	–
	0·230	–464	692	64·5	0·645
	1·149	–456	540	72·3	0·723
	2·299	–453	401	79·4	0·794
	5·747	–449	240	87·7	0·877
	11·494	–442	076	96·1	0·961
50	0·5 M H_2SO_4	–454	5415	–	–
	0·230	–448	1652	69·5	0·695
	1·149	–443	1202	77·8	0·778
	2·299	–439	899	83·4	0·834
	5·747	–435	514	90·5	0·905
	11·494	–431	146	97·3	0·973
60	0·5 M H_2SO_4	–448	8556	–	–
	0·230	–445	1506	82·4	0·824
	1·149	–440	1258	85·3	0·853
	2·299	–434	898	89·5	0·895
	5·747	–428	530	93·8	0·938
	11·494	–419	171	98·0	0·980

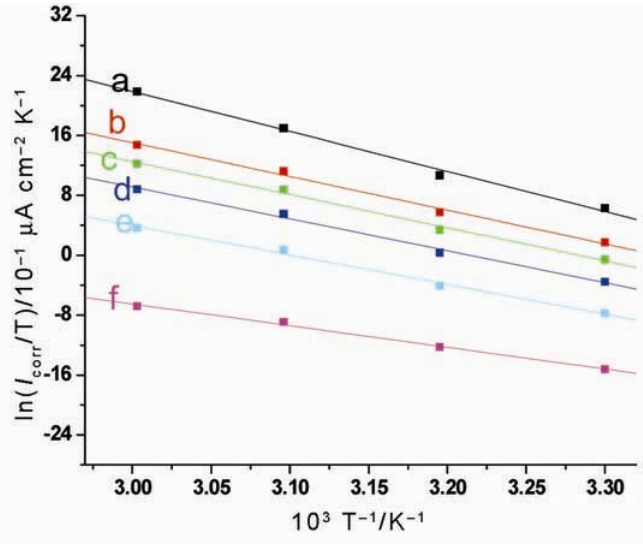

Figure 10. Arrhenius plots of $\ln(I_{corr}/T)$ vs $1/T$ at different concentrations of DHBTPH: (a) 1 M HCl, (b) 1 M HCl + $0{\cdot}230 \times 10^{-4}$, (c) 1 M HCl + $1{\cdot}149 \times 10^{-4}$, (d) 1 M HCl + $2{\cdot}299 \times 10^{-4}$, (e) 1 M HCl + $5{\cdot}747 \times 10^{-4}$ and (f) 1 M HCl + $11{\cdot}494 \times 10^{-4}$ M.

decrease in disordering takes place on going from reactants to the activated complex (Marsh 1988; Bentiss *et al* 2005).

3.4 *Application of adsorption isotherm*

In the temperature range studied, the best correlation between the experimental results and the isotherm functions was obtained using Langmuir adsorption isotherm. The Langmuir isotherm for monolayer chemisorption is given by the following equation (Agrawal and Namboodhiri 1990)

$$\frac{\theta}{1-\theta} = KC_{inh}. \tag{8}$$

Rearranging this equation gives

$$\frac{C_{inh}}{\theta} = \frac{1}{K} + C_{inh}, \tag{9}$$

where θ is the degree of surface coverage, C_{inh} the inhibitor concentration in the electrolyte and K the equilibrium constant of the adsorption process. The correlation coefficient (R^2) was used to choose the isotherm that best fit experimental data (table 7). The plot of C_{inh}/θ against C_{inh} of DHBTPH in 1 M HCl gives a straight line as shown in figure 11. Similar plots were obtained in case of DHBTPH in 2 M HCl, 0·5 M H_2SO_4 and 1 M H_2SO_4. It is found that all the linear correlation coefficients are close to 1. These isotherms conform to Langmuir's type, suggesting monolayer chemisorption of DHBTPH. From the in-

Table 5. Electrochemical parameters and the corresponding inhibition efficiencies at various temperatures studied for mild steel in 1 M H_2SO_4 containing different concentrations of DHBTPH.

Temp. (°C)	Inhibitor conc. (10^{-4} M)	E_{corr} vs SCE (mV)	I_{corr} (μAcm^{-2})	*IE* (%)	θ
30	1 M H_2SO_4	–480	2138	–	–
	0·230	–474	915	57·2	0·572
	1·149	–469	759	64·5	0·645
	2·299	–458	603	71·8	0·718
	5·747	–446	447	79·1	0·791
	11·494	–438	291	86·4	0·864
40	1 M H_2SO_4	–455	4489	–	–
	0·230	–451	1818	59·5	0·595
	1·149	–447	1499	66·6	0·666
	2·299	–441	1181	73·7	0·737
	5·747	–432	862	80·8	0·808
	11·494	–420	543	87·9	0·879
50	1 M H_2SO_4	–446	11970	–	–
	0·230	–438	4441	62·9	0·629
	1·149	–435	3627	69·7	0·697
	2·299	–425	2813	76·5	0·765
	5·747	–420	1999	83·3	0·833
	11·494	–412	1185	90·1	0·901
60	1 M H_2SO_4	–443	17314	–	–
	0·230	–435	5610	67·6	0·676
	1·149	–430	4536	73·8	0·738
	2·299	–421	3463	80·0	0·800
	5·747	–414	2389	86·2	0·862
	11·494	–405	1316	92·4	0·924

Table 6. The value of activation parameters, E_a, ΔH_a^0 and ΔS_a^0 for mild steel in acid media in the absence and presence of different concentrations of DHBTPH.

Inhibitor conc. (10^{-4} M)	E_a (kJ mol^{-1})	ΔH_a^0 (kJ mol^{-1})	ΔS_a^0 (J mol^{-1} K^{-1})
1 M HCl	46·99	44·35	–46·31
0·230	40·09	37·45	–72·71
1·149	39·38	36·74	–76·94
2·299	38·14	35·50	–83·46
5·747	35·43	32·79	–95·89
11·494	26·70	24·06	–130·81
2 M HCl	52·84	50·21	–22·38
0·230	50·31	47·67	–34·80
1·149	49·99	47·35	–37·61
2·299	49·47	46·83	–41·63
5·747	47·71	45·07	–50·53
11·494	45·31	42·67	–62·52
0·5 M H_2SO_4	60·63	57·99	4·06
0·230	40·24	37·60	–70·36
1·149	39·50	36·86	–74·61
2·299	39·27	36·63	–77·93
5·747	35·18	32·54	–94·93
11·494	33·02	30·38	–111·34
1 M H_2SO_4	61·03	58·39	11·6
0·230	53·34	50·70	–20·68
1·149	52·62	49·98	–24·59
2·299	51·49	48·85	–30·20
5·747	49·48	46·84	–39·30
11·494	44·79	42·15	–58·24

Table 7. Thermodynamic parameters for DHBTPH adsorption on mild steel in different acid media and temperatures.

Acid media	Temp (°C)	$K(M^{-1})$	R^2	ΔG^0_{ads} (kJ mol^{-1})	ΔH^0_{ads} (kJ mol^{-1})	ΔS^0_{ads} (J mol^{-1} K^{-1})
1 M HCl	30	10525	0·996	–33·45	12·31	150·65
	40	11290	0·997	–34·74		
	50	12950	0·997	–36·22		
	60	16331	0·998	–37·98		
2 M HCl	30	12021	0·998	–33·79	4·58	126·50
	40	12368	0·998	–34·98		
	50	12933	0·998	–36·22		
	60	14185	0·998	–37·59		
0·5 M H_2SO_4	30	21207	0·998	–35·22	27·15	204·97
	40	24857	0·999	–36·80		
	50	32135	0·999	–38·66		
	60	56701	1·000	–41·43		
1 M H_2SO_4	30	22413	0·999	–35·36	9·81	148·86
	40	24135	0·999	–36·72		
	50	26916	0·999	–38·19		
	60	31841	0·999	–39·83		

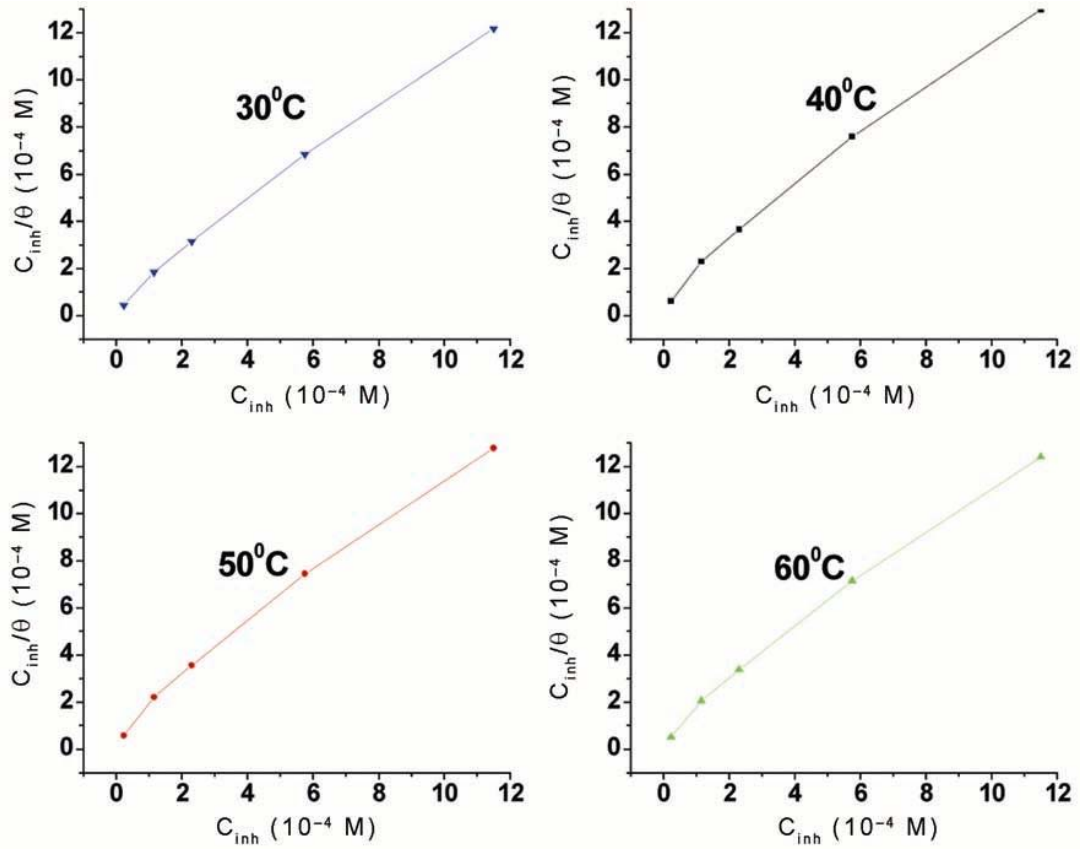

Figure 11. Langmuir's adsorption isotherms for DHBTPH on the surface of mild steel in 1 M HCl at different temperatures.

tercepts of the straight lines, C_{inh}/θ-axis, K values were calculated and are given in table 7.

The constant of adsorption, K, is related to the standard free energy of adsorption, ΔG^0_{ads}, with the following equation:

$$K = \frac{1}{55{\cdot}5}\exp\left(\frac{-\Delta G^0_{ads}}{RT}\right). \quad (10)$$

The value, 55·5, in the above equation is the concentration of water in solution in mol L^{-1} (Bouklah *et al* 2006). From the above equation the standard free of adsorption (ΔG^0_{ads}) can be calculated.

A plot of (ΔG^0_{ads}) vs T in figure 12 gave the heat of adsorption (ΔH^0_{ads}) and the standard entropy (ΔS^0_{ads}) according to the thermodynamic basic equation, $\Delta G^0_{ads} = \Delta H^0_{ads} - T\Delta S^0_{ads}$. Figure 12 clearly shows the good dependence of

ΔG^0_{ads} on T, indicating the good correlation among thermodynamic parameters. The thermodynamic data obtained from DHBTPH using the adsorption isotherm are depicted in table 7. The negative value of ΔG^0_{ads} ensure the spontaneity of the adsorption process and stability of the adsorbed layer on the steel surface. The calculated ΔG^0_{ads} values are closer to –40 kJ mol^{-1} (table 7) indicating that the adsorption mechanism of the DHBTPH on steel in studied acid media was typical of chemisorption (Yurt *et al* 2005). The unshared electron pairs in sulphur, nitrogen as well as in oxygen may interact with *d*-orbitals of steel to provide a protective chemisorbed film (Bentiss *et al* 2000).

The values of thermodynamic parameter for the adsorption of inhibitors can provide valuable information about the mechanism of corrosion inhibition. In the presented case, the calculated values of ΔH^0_{ads} for the adsorption of DHBTPH in 1 M HCl, 2 M HCl, 0·5 M H_2SO_4 and 1 M H_2SO_4 is 12·31, 4·58, 27·15 and 9·81 kJ mol^{-1}, respectively, indicating that this inhibitor can be considered chemically adsorbed (Durnie *et al* 1999). The high value of ΔH^0_{ads} in the case of DHBTPH in 1 M HCl and 0·5M H_2SO_4 indicated that this is more strongly adsorbed on the steel surface. This is in good agreement with the results obtained from weight-loss, EIS and Tafel measurements.

The ΔS^0_{ads} values in the presence of DHBTPH in 1 M HCl, 2 M HCl, 0·5 M H_2SO_4 and 1 M H_2SO_4 are large and positive, meaning that an increase in disordering takes place in going from reactants to the metal-adsorbed species reaction complex (Banerjee and Malhotra 1992).

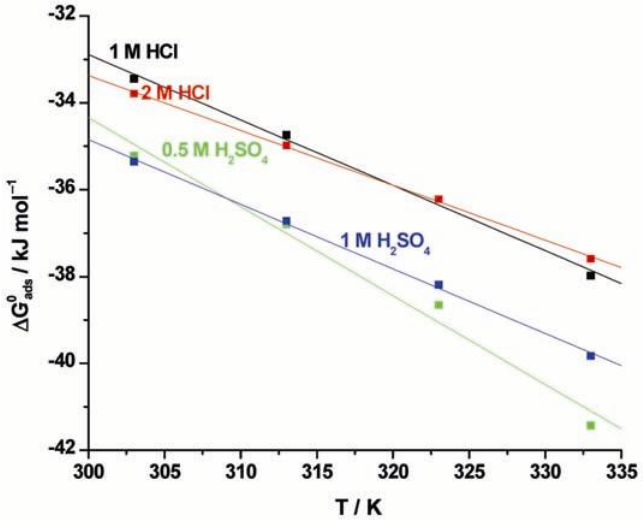

Figure 12. Variation of ΔG^0_{ads} vs T on mild steel in acid media containing DHBTPH.

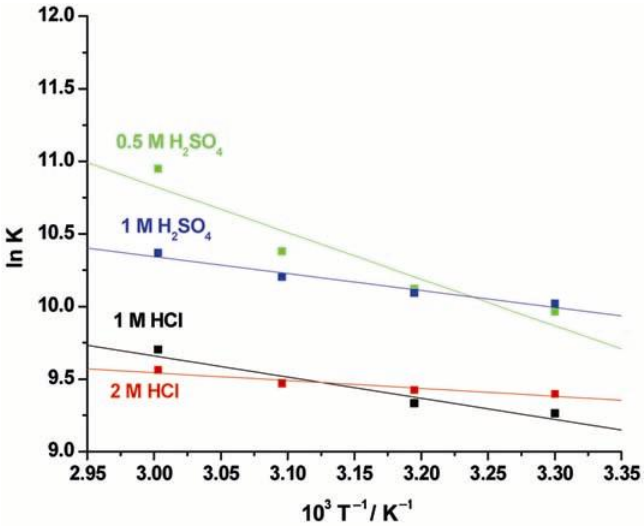

Figure 13. Van't Hoff plots for the mild steel in DHBTPH in acid media.

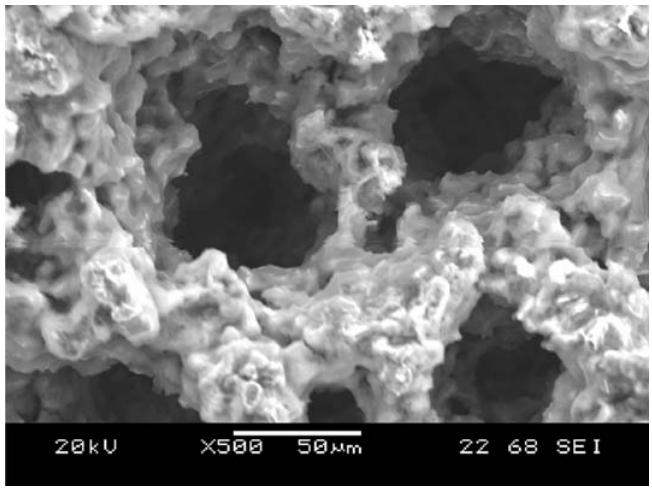

Figure 14. SEM image of surface of mild steel after immersion for 24 h in 1 M HCl at 30°C (Magnification, X500).

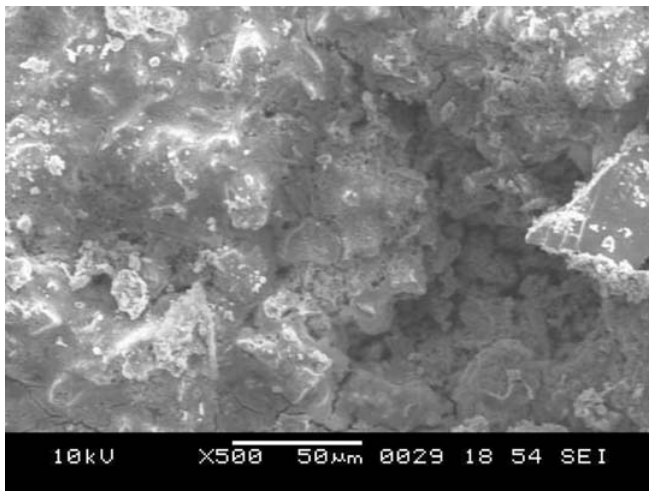

Figure 15. SEM image of surface of mild steel after immersion for 24 h in 0·5 M H_2SO_4 at 30°C (Magnification, X500).

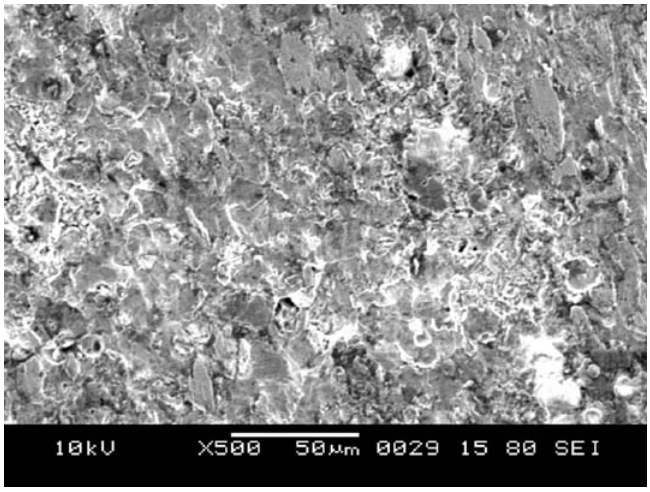

Figure 16. SEM image of surface of mild steel after immersion for 24 h in 1 M HCl at 30°C in presence of $11{\cdot}494 \times 10^{-4}$ M. DHBTPH (Magnification, X500).

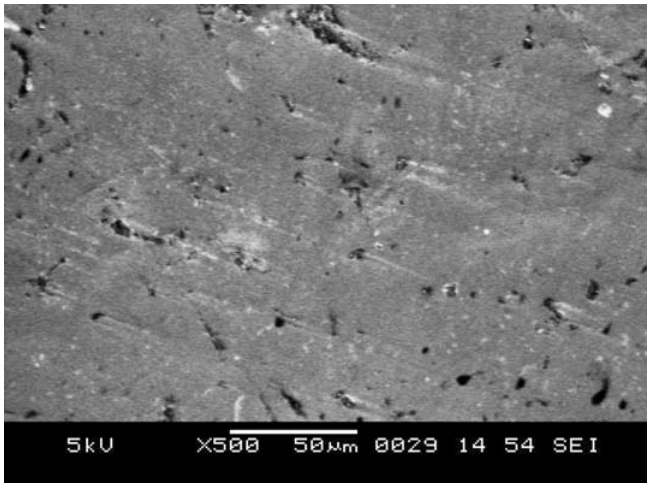

Figure 17. SEM image of surface of mild steel after immersion for 24 h in 0·5 M H_2SO_4 at 30°C in presence of $11{\cdot}494 \times 10^{-4}$ M DHBTPH (Magnification, X500).

The following integrated version of the Van't Hoff equation can also be used to obtain ΔH^0_{ads} values (Tang *et al* 2006)

$$\ln K = -\frac{\Delta H^0_{ads}}{RT} + \text{constant}. \quad (11)$$

Figure 13 shows the plot of $\ln K$ vs $1/T$ for DHBTPH in 1 M HCl which gives straight lines with slopes $(-\Delta H^0_{ads}/R)$ and intercepts $(\Delta S^0_{ads}/R + \ln 1/55{\cdot}5)$. Similar plots were obtained in case of DHBTPH in different acid media. The calculated ΔH^0_{ads} values using the Van't Hoff equation are 12·12, 4·51, 26·68 and 9·70 kJ mol^{-1} for 1 M HCl, 2 M HCl, 0·5 M H_2SO_4 and 1 M H_2SO_4, respectively, confirming the endothermic behaviour of the adsorption of these inhibitors on the steel surface, therefore, the chemisorptions process. Values of ΔH^0_{ads} obtained by both the methods are in good agreement. Moreover, the deduced ΔS^0_{ads} values of 150·05, 126·26, 203·47 and 148·50 J mol^{-1} K^{-1} for DHBTPH in 1 M HCl, 2 M HCl, 0·5 M H_2SO_4 and 1 M H_2SO_4, respectively are very close to that obtained in table 7.

3.5 *Scanning electron microscopy*

The SEM micrographs of the corroded mild steel in the presence of 1 M HCl and 0·5 M H_2SO_4 solutions are shown in figures 14 and 15. The faceting seen in the figures was a result of pits formed due to the exposure of mild steel to the acid. The influences of the inhibitor addition ($11{\cdot}494 \times 10^{-4}$ M) on the mild steel in 1 M HCl and 0·5 M H_2SO_4 solutions are shown in figures 16 and 17. The faceting observed in figures 14 and 15 disappeared and the surface was free from pits and it was smooth. It can be concluded from figures 14–17 that corrosion does not occur in presence of inhibitor and hence corrosion was inhibited strongly when the inhibitor was present in the acid media (Keera 2003).

4. Conclusions

(I) Reasonably good agreement was observed between the data obtained from the weight-loss, electrochemical impedance spectroscopy and potentiodynamic polarization techniques.
(II) DHBTPH suppressed the anodic reaction to greater extents than the cathodic one; these observations suggest that DHBTPH behaves mainly as anodic inhibitor in the studied acid. The inhibition efficiency trend in different acid media was in the decreasing order 0·5 M H_2SO_4 > 1 M HCl > 1 M H_2SO_4 > 2 M HCl.
(III) *%IE* of DHBTPH was temperature-dependent and their addition led to a decrease of the activation corrosion energy in all the studied acid media.
(IV) The thermodynamics parameters reveal that the inhibition of corrosion by DHBTPH is due to the formation of a chemisorbed film on the metal surface.
(V) Adsorption of DHBTPH was found to follow the Langmuir's adsorption isotherm.

Acknowledgements

The authors are thankful to the Head, Chemistry Department, NITK and Head, SeQuent Scientific Ltd., Mangalore, for their encouragement and necessary laboratory facilities.

References

Abd El-Rehim S S, Ibrahim M A M and Khaled K F 1999 *J. Appl. Electrochem.* **29** 593

Agrawal R and Namboodhiri T K G 1990 *Corros. Sci.* **30** 37
Allais, Andre and Meier Jean 1969 (Roussel-UCLAF) Ger. Offen. 1815467
Ammar I A and Khorafi F M El 1973 *Werkst. Korros.* **24** 702
Banerjee G and Malhotra S N 1992 *Corrosion* **48** 10
Bentiss F, Traisnel M and Lagrenee M 2000 *Corros. Sci.* **42** 127
Bentiss F, Traisnel M and Lagrenee M 2001 *J. Appl. Electrochem.* **31** 41
Bentiss F, Lagrenee M, Mehdi B, Mernari B, Traisnel M and Vezin H 2002 *Corrosion* **58** 399
Bentiss F, Lebrini M and Lagrenee M 2005 *Corros. Sci.* **47** 2915
Bouklah M, Hammouti B, Lagrenee M and Bentiss F 2006 *Corros. Sci.* **48** 2831
Durnie W, Marco R D, Jefferson A and Kinsella A B 1999 *J. Electrochem. Soc.* **146** 1751
Emregul Kaan C, Kurtaran Raif and Atakol Orhan 2003 *Corros. Sci.* **45** 2803
Foad E E and Sherbini E1 1999 *Mater. Chem. Phys.* **60** 286
Ivanov E S 1986 *Inhibitors for metal corrosion in acid media* (Moscow: Metallurgy)
Juttner K 1990 *Electrochim. Acta* **35** 1501
Keera S T 2003 *J. Sci. Ind. Res.* **62** 188
Khaled F, Babic-Samardzija K and Hackerman N 2004 *J. Appl. Electrochem.* **34** 697
Khamis E 1990 *Corrosion* **46** 6
Marsh J 1988 *Advanced organic chemistry* (New Delhi: Wiley Eastern) 3rd ed.
McCafferty E and Hackerman N 1972 *J. Electrochem. Soc.* **119** 146
Mehaute A H and Grepy G 1989 *Solid State Ionics* **9–10** 17
Mora-Mendoza J L, Chacon-Nava J G, Zavala-Olivares G, Gonzalez-Nunez M A and Turgoose S 2002 *Corros. Eng.* **58** 608
Muralidharan S, Quraishi M A and Iyer S V K 1995 *Corros. Sci.* **37** 1739
Popova A, Christov M, Raicheva S and Sokolova E 2004 *Corros. Sci.* **46** 1333
Quraishi M A and Jamal D 2002 *J. Appl. Electrochem.* **32** 425
Quraishi M A, Jamal D and Singh R N 2002 *Corrosion* **58** 201
Reinhard G and Rammet U 1985 in *Proceedings 6th European symposium on corrosion inhibitors* (Ferrara: Ann. University) p. 831
Rengamani S, Muralidharan S, Anbu Kulamdainathan M and Venkatakrishna Iyer S 1994 *J. Appl. Electrochem.* **24** 355
Stoynov Z B, Grafov B M, Savova-Stoynova B and Elkin V V 1991 *Electrochemical impedance* (Moscow: Nauka)
Tang Libin, Li Xueming and Li Lin 2006 *Mater. Chem. Phys.* **97** 301
Vishwanatham S and Anil Kumar 2005 *Corros. Rev.* **23** 181
Wang Hui-Long, Liu Rui-Bin and Xin Jian 2004 *Corros. Sci.* **46** 2455
Yurt A, Bereket G, Kivrak A, Balaban A and Erk B 2005 *J. Appl. Electrochem.* **35** 1025
Zor Sibel, Dogan Pinar and Yazici Birgul 2005 *Corros. Rev.* **23** 217